The impact of varying spatial resolution of climate models on future rainfall simulations in the Pra River Basin (Ghana)

Article *in* Journal of Water and Climate Change · July 2019

DOI: 10.2166/wcc.2019.258

CITATIONS
9

READS
143

5 authors, including:

Enoch Bessah
Kwame Nkrumah University Of Science and Technology
40 PUBLICATIONS **100** CITATIONS
SEE PROFILE

A.O. Raji
University of Ibadan
73 PUBLICATIONS **1,352** CITATIONS
SEE PROFILE

Olalekan Taiwo
University of Ibadan
44 PUBLICATIONS **365** CITATIONS
SEE PROFILE

Sampson K. Agodzo
Kwame Nkrumah University Of Science and Technology
57 PUBLICATIONS **418** CITATIONS
SEE PROFILE

The impact of varying spatial resolution of climate models on future rainfall simulations in the Pra River Basin (Ghana)

Enoch Bessah, Abdulganiy O. Raji, Olalekan J. Taiwo, Sampson K. Agodzo and Olusola O. Ololade

ABSTRACT

This work compares future projections of rainfall over the Pra River Basin (Ghana) using data from five climate models for the period 2020–2049, as referenced to the control period 1981–2010. Bias-correction methods were applied where necessary and models' performances were evaluated with Nash–Sutcliffe Efficiency, root-mean-square error and coefficient of determination. Standardised Anomaly Index (SAI) was used to determine variability. The onset and cessation dates and length of the rainy season were determined by modifying the Walter–Olaniran method. The ensemble means of the models projected a 1.77% decrease in rainfall. The SAI showed that there would be drier than normal years with the likelihood of drought occurrence in 2021, 2023, 2031 and 2036. The findings showed that high-resolution models (≤25 km) were more capable of simulating rainfall at the basin scale than mid-resolution models (26–150 km) and projected a 20.13% increase. Therefore, the rainfall amount is expected to increase in the future. However, the projected increase in the length of the dry season by the ensemble of the models suggested that alternative sources of water would be necessary to supplement rainfed crop production for food security.

Key words | climate change, Ghana, Pra River Basin, rainfall modelling, RCMs, SDSM

Enoch Bessah (corresponding author)
Pan African University, Institute of Life and Earth Sciences (Including Health and Agriculture), University of Ibadan,
Oyo State, Nigeria
E-mail: *ebessah0180@stu.ui.edu.ng*

Abdulganiy O. Raji
Department of Agricultural and Environmental Engineering,
University of Ibadan,
Oyo State, Nigeria

Olalekan J. Taiwo
Department of Geography,
University of Ibadan,
Oyo State, Nigeria

Sampson K. Agodzo
Department of Agricultural and Biosystems Engineering,
Kwame Nkrumah University of Science and Technology, PMB,
Kumasi, Ghana

Olusola O. Ololade
Centre for Environmental Management,
University of the Free State,
Bloemfontein 9300,
Republic of South Africa

INTRODUCTION

Recently, the impact of climate change on water resources and its services are increasingly evident, especially in developing countries (IPCC 2007, 2014; Boon & Ahenkan 2012; Obuobie *et al.* 2012; Cubasch *et al.* 2013). Projections indicate that global temperature will continue to increase and will impact on rainfall patterns via its effects on evaporation and evapotranspiration from land, water and plants into the atmosphere (Marcé *et al.* 2010; López-Moreno *et al.* 2011). This will lead to natural hazards like flooding and droughts, which may not have a severe impact on populations with better economic and political stability, and improved agricultural technology (Davis *et al.* 2015). However, the impact will be significant in Africa due to poverty and political instability, amongst others (Burke *et al.* 2009; Niang *et al.* 2014). As a result, poverty is expected to increase, food will be scarcer and development will be less sustainable (UNEP 2002; Bo *et al.* 2004; FAO 2009; Serdeczny *et al.* 2016; Welborn 2018). A major determinant of agricultural production globally is rainfall. Climate change has affected the seasonal and annual characteristics of rainfall (Mawunya *et al.* 2011) leading to fluctuations in crop yields across many parts of the world (Brahic 2007;

doi: 10.2166/wcc.2019.258

Rasul *et al.* 2011; Knox *et al.* 2013; Hatfield & Prueger 2015; UNEP 2017).

Obuobie *et al.* (2012) used the fourth-generation European Centre Hamburg Model (ECHAM4) and the Commonwealth Scientific and Industrial Research Organization, Australia (CSIRO) joint model and projected a decrease in rainfall by 12.3% and 17.8% by 2020 (2006–2035) and 19.6% and 25.9% by 2050 (2036–2065) in the White Volta and Pra basins, respectively. In addition, the Fourth Assessment Report (AR4) climate change scenarios of central Ghana by 2050 indicated a decrease of 10% in precipitation (WRC 2012). Nutsukpo *et al.* (2013) assessed precipitation change over Ghana using the A1B scenario with four downscaled general circulation models (GCMs). Two of the models, namely the National Meteorological Research Center – Climate Model 3 and ECHAM5 projected an increase of precipitation in the extreme southern part and south-eastern part of the country, respectively. The CSIRO Mark 3 projected a general decrease in precipitation, while the Model for Interdisciplinary Research on Climate (MIROC 3.2) projected increasing precipitation in the north and decrease in the south of Ghana (Nutsukpo *et al.* 2013). Projections of precipitation are influenced by the resolution of models, their associated uncertainties and bias of downscaling (Souvignet *et al.* 2010). There is a need to assess the climate impact with multiple climate data using different resolution models to get the moderate scenario for the Pra River Basin, which is dominated by tuber crop and cash crop production as well as the potential damming site in Ghana (WRC 2012; Nutsukpo *et al.* 2013).

Agriculture and its related economies employ more than 63% of the population in the basin with cocoa farming, the main commercial crop, which accounts for over 70% of household income (WRC 2012). Cocoa is a major export agricultural product, which contributed to 8.2% of the total Agriculture GDP of Ghana in 2010 (MoFA 2011). Peasant farmers in the basin mostly cultivate food crops like cassava, maize, plantain and especially tuber crops, which ensures national food security (Nutsukpo *et al.* 2013). Unfortunately, agriculture is mainly rainfed, with few irrigation technologies emerging from government and international projects (WRC 2012). Water availability to sustain the livelihood of farmers and the economy of the nation is critical due to the changing climate. Moreover, about six of the potential hydro-dam sites are located in the basin (Ahiataku-Togobo 2014). Knowledge of future rainfall in the study area is currently necessary for policy and adaptation planning.

The aim of this study was to project rainfall variability and change in the period 2020–2049 with five different climate models at different spatial resolutions under the Representative Concentration Pathway 4.5 (RCP4.5) emission scenario for the Pra River Basin of Ghana. Rainfall onset, cessation and length of the rainy season (LRS) for the observed (1981–2010) and future period (2020–2049) were also determined.

METHODS

Study area

The Pra River Basin is the largest south-western drainage basin in Ghana, covers an area of 23,321 km^2 and lies between latitudes 4°58′ N and 7°11′ N and longitudes 0°25′ W and 2°13′ W, as shown in Figure 1 (Kusimi *et al.* 2015). It stretches to the Gulf of Guinea at Shama town in the Western Region. The annual mean temperature ranges between 26 °C and 27 °C (Bessah *et al.* 2018). The basin supplies water to the capitals of Ashanti, Western and Central Region for both domestic and industrial uses. About 41 districts and over 1,300 towns also benefit from the water sources in the basin (Kusimi *et al.* 2015). Water resources were available all year round until the increase in anthropogenic activities such as agricultural expansion, mining (legal and illegal) and logging, which are adversely degrading the quality of water resources in the basin (WRC 2012). The basin has a bi-modal rainfall pattern with the major rains occurring between May and June and the minor rains occurring around September to October (Dickson & Benneh 1995). The moist south-west monsoon is a major driver of the rainfall pattern within the basin. The dry season occurs mainly from November after the cessation of the minor rains to March (Dickson & Benneh 1995). Some of the local physical features such as basin topography (elevation ranging from −2 to 842 m), the natural meteorite lake (Lake Bosomtwe) and land cover change of

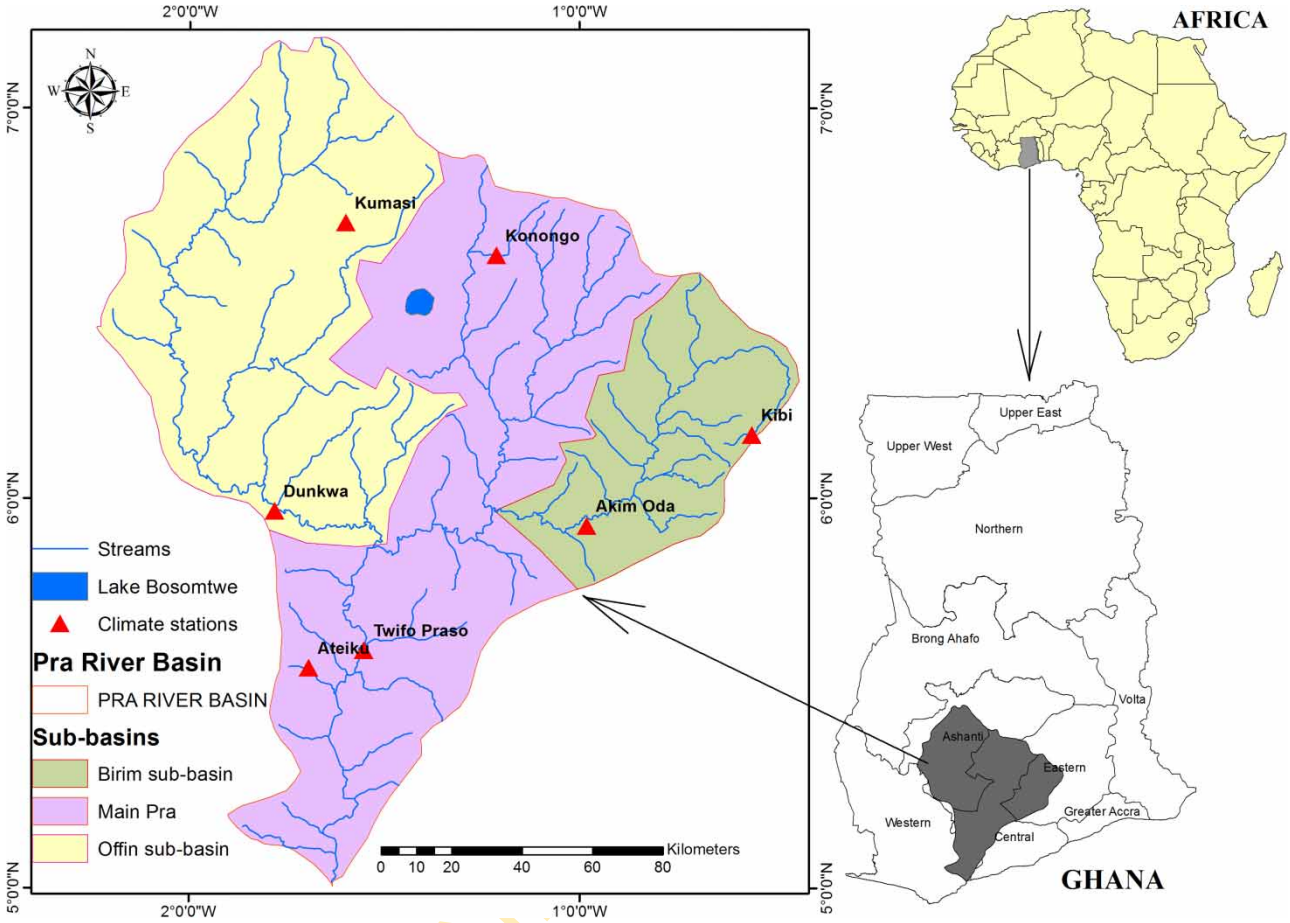

Figure 1 | Map of the Pra River Basin.

the semi-deciduous forest contribute to rainfall variability in the basin. These features are linked to major driving forces such as sea surface temperature and relative humidity (Nicholson & Webster 2007; Ambrosino 2011; Goodess *et al.* 2011).

Dataset description

Historical daily rainfall data from seven operational climate stations (Table 1) out of the 30 stations identified in the Pra River Basin (Figure 1) with minimal missing data were

Table 1 | Characteristics of selected climate stations

Station ID	Station name	Date opened	Latitude	Longitude	Altitude (m)	Region
18026ATI	ATIEKU	01-09-51	05° 34′ N	01° 42′ W	106.6	WESTERN
17015DUN	DUNKWA ON OFFIN	01-01-44	05° 58′ N	01° 47′ W	158.6	CENTRAL
23023TWI	TWIFO PRASO	01-01-37	05° 36′ N	01° 33′ W	76	CENTRAL
21020KIB	KIBI	01-01-12	06° 10′ N	00° 33′ W	274.2	EASTERN
21088ODA	AKIM ODA	11-09-72	05° 56′ N	00° 59′ W	139.4	EASTERN
19007KON	KONONGO	01-03-34	06° 37′ N	01° 13′ W	243.7	ASHANTI
17009KSI	KUMASI AIRPORT	01-01-45	06° 43′ N	01° 36′ W	286.3	ASHANTI

acquired from the Ghana Meteorological Agency (GMet). Amelia package in R software was used to fill gaps in data for the reference period 1981–2010 to enhance the performance assessment of the models at equal conditions of station data (Arguez *et al.* 2012). Climate stations that had missing data were Atieku (2.5%), Kononga (0.8%), Dunkwa (1.1%), Kibi (14.2%) and Twifo Praso (4.7%). Rainfall data were subjected to quality control in RClimdex after filling the gaps to identify outliers and erroneous data such as negative rainfall values which were then removed (Aguilar *et al.* 2009). Table 1 presents the characteristics of the seven climate stations used in this study. The emission scenario used for analysis comprised the Representative Concentration Pathways 4.5 W/m^2 mitigation scenario. The RCP4.5 represented B1 of the Fourth Assessment Report (AR4) Special Report on Emissions Scenarios (SRES) (Fenech *et al.* 2007; IPCC 2007; Cubasch *et al.* 2013). Although tropical West Africa is reported to be a hotspot of climate change under both RCP4.5 and RCP8.5 for the late 2030s to early 2040s (Diffenbaugh & Giorgi 2012; Mora *et al.* 2013), the goal of the United Nations Framework Convention on Climate Change through policies such as the Kyoto protocol and Paris agreement is to achieve the emission target under the RCP 4.5 scenario and even lower (Lomborg 2016; Muthee *et al.* 2018).

Table 2 presents the characteristics of the GCMs and their regional climate models (RCMs) data, which were used. The model validation method of Fenech *et al.* (2007), which employs the region of first standard deviation (1xStdev) and second standard deviation (2xStdev), was used to choose CanESM2 and IPSL models (full name of the models described in Table 2) as best models over the Pra River Basin, out of 43 models from the Intergovernmental Panel on Climate Change (IPCC) Fifth Assessment Report (AR5) (detailed in section 'Description of AR5 GCMs data validation'). The RCM of the two models, downloaded from the Coordinated Regional Climate Downscaling Experiment (CORDEX) site, was the Rossby Centre regional atmospheric model (RCA4) by the Swedish Meteorological and Hydrological Institute (SMHI). From the geoportal of West African Science Service Centre on Climate Change and Adapted Land Use (WASCAL), the Weather Research and Forecasting Model (WRF) of GFDL and HadGEM2 (detailed in Table 2) were downloaded (Heinzeller *et al.* 2016a). High temporal (3 hrs) and spatial (12 km) resolution were some of the strengths of the WRF model, while its forecast length of 48 h and sensitivity to atmospheric conditions was classified as a weakness (Heinzeller 2019). The GFDL-ESM2M and HADGEM2-ES represent extreme wet and dry conditions, respectively, over West Africa (Heinzeller 2019). The SMHI-RCA4 CORDEX model in comparison with previous versions showed an improvement in the resolution from 50 to 44 km with a downside of overestimating precipitation based on a test result over Europe (Samuelsson *et al.* 2011). Statistical Downscaling Model – Decision Centric (SDSM-DC) version 5.2 with a resolution of 2 m (Wilby *et al.* 2002; Wilby *et al.* 2014) was the fifth model acquired from the SDSM website. The SDSM combines a stochastic weather generator and multiple linear regression in downscaling from the National Center for Environmental Prediction (NCEP) grids at a $2.5^\circ \times 2.5^\circ$ resolution for each station. The following steps, namely screen variables selection, calibration, validation, weather generation and

Table 2 | Description of climate models

Acronym	Originating group	Country	GCM name	RCM	Resolution	Days in a year	Reference
GFDL	NOAA Geophysical Fluid Dynamics Laboratory	USA	GFDL-ESM2M	WRF	12 km	365	Heinzeller *et al.* (2016a)
HadGEM	Hadley Centre for Climate Prediction and Research	UK	HadGEM2-ES	WRF	12 km	360	Heinzeller *et al.* (2016b)
IPSL	Institut Pierre Simon Laplace	France	IPSL-CM5A-MR	SMHI-RCA4	44 km	365	Giorgi *et al.* (2009); Déandreis *et al.* (2014)
CCCma	Canadian Centre for Climate Modeling and Analysis	Canada	CCCma-CanESM2	SMHI-RCA4	44 km	365	Giorgi *et al.* (2009); Chylek *et al.* (2011)
SDSM	Wilby & Dawson (2013)	UK	NCEP	SDSM-DC	2 m	366	Wilby & Dawson (2013)

scenario generation, were duly followed in the SDSM-DC 5.2. The calibration and validation of SDSM were done with NCEP predictors as the daily large-scale atmospheric variables and observed records at each station as *predictands*. The model names GFDL-ESM2M, HadGEM2-ES, IPSL-CM5A-MR, CCCma-CanESM2 and SDSM-DC are referred to hereafter as GFDL, Hadgem, IPSL, CanESM and SDSM, respectively (Table 2). A spatial resolution of <25 km, 26–150 km and >150 km was referred to as high, mid and low resolution, respectively, in this study, especially in the presentation of results and conclusion.

Description of AR5 GCMs data validation

Annual historical (1981–2010) and future (2006–2099) temperatures (2 m above sea level) and precipitation simulations for each station (point assessment) and also over the Pra River Basin (area assessment) for the 43 GCMs in AR5 were downloaded in the CSV format through scatterplots on the UPEI database. The UPEI database is one of the services provided by the UPEI Climate Lab to make climate baseline and future datasets available and accessible. Annual observation values for the same historical period from NCEP reanalysis datasets for each of the stations were also downloaded through the same medium. The difference between GCMs historical simulations and NCEP observed reanalysis data for temperature and precipitation were plotted as XY scatter graphs (Fenech *et al.* 2007). The zone of acceptability was estimated by calculating the standard deviation (1xStdev) of the XY scatter plot data and doubling it to get zone 2 (2xStdev). The zones were then drawn on the XY scatter plots to determine the type and number of models, which fell within the acceptable zone for the validation of the GCMs results for the study area. Graphs showing changes in each future period [2020s (2011–2040), 2050s (2041–2070) and 2080s (2071–2099)] were produced from the maximum, minimum, mean (ensemble) and validated (mean of models that fell within the acceptable zone) of the annual simulations of the GCMs. The two most recurring validation GCMs at the seven climate stations and in the area analysis over the basin available on CORDEX Africa-domain were CCCma-CanESM2 and IPSL-CM5A-MR (Table 2).

Data analysis

The R software (Packages: ncdf.tools, ncdf and raster) was used to extract RCMs daily rainfall using the geographical coordinates of the seven climate stations. The historical simulation of the WRF model was from 1980 to 2009, and that of SMHI-RCA4 ended in 2005. Therefore, the RCP4.5 run for 2006–2010 was added to its historical simulation to obtain the 1981–2010 simulation to enable performance evaluation of the model with the observed data (Dosio & Panitz 2016). All analyses of the WRF model were based on the reference period 1980–2009 for all stations. Since bias-correction was not an objective in this study, only RCMs output that fell outside the acceptable range of the time-series-based metric after the performance evaluation were bias-corrected (Bessah *et al.* 2018). Bias-correction was necessary for these RCMs to reduce the uncertainty of the ensemble mean results for the basin. This was to make the findings applicable for policy and climate change adaptation planning. The linear scaling method and the double quantile mapping bias-correction methods were used wherever necessary (Teutschbein & Seibert 2012). The linear scaling method matched the monthly mean of corrected values to the observed, while the double quantile mapping corrected the variations errors of data from the mean (Lenderink *et al.* 2007; Teutschbein & Seibert 2012). The difference between the simulated and observed daily values corrected by the mean value within a month for the whole period of assessment formed the Linear scaling approach. Cumulative distribution functions of both observed and modelled data were used to determine interpolation between the points presented by a quantile-quantile scatter plot (Canon *et al.* 2015). The time-series-based metrics employed to evaluate the performance of the models were Nash–Sutcliffe Efficiency (NSE), root-mean-square error (RMSE) and coefficient of determination (R^2) (Moriasi *et al.* 2007). That is, the levels of agreement between the historical rainfall simulation of each model and the observed rainfall records for each station for the same period were calculated by NSE, RMSE and R^2. The position of each model within the acceptable range of the time-series metrics [NSE (0.0–1.0), RMSE (0 = perfect fit, the lower the better) and R^2 (>0.50)] and the mean range across the seven stations determined the ability of a model in simulating

rainfall over the basin (Moriasi *et al.* 2007). During the grading of the models' abilities, a low value in any of the time-series-based metric for the performance assessment without bias-correction was higher than bias-corrected. Equal weights of 5 and 1 representing the highest and lowest value amongst the five models of each metric per stations were computed. The weights were summed across the three metrics and seven stations to determine the overall metric for each model over the study area. The Standardised Anomaly Index (SAI) of rainfall was determined by the Hadgu *et al.* (2013) formula [Equation (1)], while the onset and cessation dates and LRS were determined by creating assumptions for the Walter–Olaniran method, described in Equation (2) (Matthew *et al.* 2017). The Walter–Olaniran method is said to perform poorly in the forest zone compared to the Savannah and Sudan-Sahel (Matthew *et al.* 2017). The modification involved the assumption that (1) a month selected for the onset date determination should have a total monthly precipitation of >50.8 mm (effective rainfall) and the succeeding month should also have the same condition and (2) the cessation date determination follows the same assumption for onset, but in this case, the month should be the preceding not the succession month. An ordinary kriging interpolation method in ArcGIS 10.3 was used to generate the spatial distribution of the rate of change in the mean annual rainfall for the period 2020–2049 with spherical semi-variogram kriging minimising interpolation errors during predictions by the variogram expressing the variation in space (Oliver & Webster 1990).

$$SAI = \frac{(x - \mu)}{\sigma} \tag{1}$$

where x is the annual/seasonal precipitation, μ is the long-term seasonal mean and σ is its standard deviation.

$$Onset/Cessation\ \ Date = \frac{D(50.8 - F)}{R} \tag{2}$$

where D is the number of days in the first month (onset) or last month (cessation) in the year with effective rain; F is the accumulated rainfall totals of previous month (for cessation it will be backward, i.e. from December) and R is the total rainfall in the first month (onset) or last month (cessation) with effective rain.

Calibration of SDSM

The analysis showed a very low partial correlation level between the station rainfall data and predictors (Table 3). The best predictors selected for rainfall calibration were direct shortwave radiation, surface lifted index, vorticity near the surface, 850 hPa and 500 hPa, surface divergence,

Table 3 | The partial correlations between the selected predictors and the observed station rainfall of SDSM model calibration for the base period 1981–2010

		Synoptic stations						
Predictor	**Description**	**Atieku**	**Dunkwa on Ofin**	**Twifo Praso**	**Akim Oda**	**Kibi**	**Kumasi**	**Konongo**
dswr	Direct shortwave radiation			−0.04				
lftx	Surface lifted index		−0.09	−0.08	−0.08	−0.10	−0.08	−0.09
p_z	Vorticity near the surface			−0.06				
p_zh	Surface divergence						0.06	
p5_z	Vorticity at 500 hPa					0.04		0.09
P8_z	Vorticity at 850 hPa		0.04					
pr_wtr	Precipitable water	0.09	0.04	0.06	0.08	0.08	0.04	0.09
prec	Precipitation total	0.08	0.06	0.05	0.04	0.06	0.06	0.06
r850	Relative humidity at 850 hPa height	0.07	−0.06	−0.04	−0.08	−0.06	−0.07	−0.08
r500	Relative humidity at 500 hPa height	0.06						
rhum	Near-surface relative humidity							0.05

precipitable water, total precipitation and relative humidity at 850 hPa and 500 hPa and near-surface relative humidity. Each station was calibrated with a minimum of four of the listed predictors with significance at a 95% confidence level. The partial correlation of rainfall as a conditional model and predictors was very low. It implied that rainfall was very difficult to predict in this zone. Rainfall as a conditional process has an intermediary process between the local weather and regional forcings that have a direct link with wet and/or dry day occurrence. The process further depends on parameters like atmospheric pressure and humidity (Wilby & Dawson 2004; Gulacha & Mulungu 2016). Therefore, rainfall downscaling has been found to be problematic and difficult compared with temperature (Hassan & Harun 2011). The results are similar to the findings of Gulacha & Mulungu (2016). The cross-validation was done at twofold, that is, the data were divided into two equal 15 years' intervals for calibration and the remaining 15 years for validation. The mean of proportion accuracy (prop correct) for validation of the model was in the range of 61–71% across the seven stations. Future climate scenarios for SDSM were generated using the mean validated projected rainfall change of the 2020s and 2050s from the 43 GCMs of the IPCC fifth assessment report (AR5) at each station (Table 4). The GCMs projections for each station were determined using the climate database of the University of Prince Edward Island (UPEI 2017; Bessah *et al.* 2018). The event threshold for rainfall modelling in SDSM was set at 0.85 (Garbutt *et al.* 1981) and the mean addition treatments of rainfall rate were employed in generating the future scenarios for 2020–2049.

RESULTS AND DISCUSSION

AR5 projection of rainfall over Pra River Basin

The Pra River Basin lies between latitude 4.94°N and 7.20°N and longitude 0.95°W and 2.65°W on the UPEI database, which was used for the extraction of the total rainfall data (Bessah *et al.* 2018). A mean rainfall rate of 3.67 mm/day was recorded for the ensemble of 43 GCMs in the fifth Assessment Report (AR5) of IPCC with a range of 1.81–7.09 mm/day for 1981–2010. The mean rainfall rate of the climate stations within the basin was 3.69 mm/day with a difference of 0.02 over the area (Table 4). Rainfall in the basin was projected to a respective increase from the base period (1981–2010) by 0.81%, 0.60% and 1.62% for the 2020s (2011–2040), 2050s (2041–2070) and 2080s (2071–2099) (Figure 2). The projected mean of the seven stations confirmed results determined for the basin area in Figure 2. However, validated results from the selected stations projected rainfall decrease of 0.62% and 1.62% for the 2050s and 2080s, respectively (Table 4). The contradictions in the results of individual stations and the basin as a whole were due to the spatial variation of rainfall within the basin.

Table 4 | AR5 Ensemble and validated precipitation rate projections of the selected stations in the Pra River Basin

	Ensemble (Mean)				Validated Mean[a]			
Climate stations	**Baseline (mm/d)**	**2020s (%)**	**2050s (%)**	**2080s (%)**	**Baseline (mm/d)**	**2020s (%)**	**2050s (%)**	**2080s (%)**
Akim Oda	3.60	1.64	2.63	4.40	3.73	2.01	1.96	0.47
Kumasi	3.92	0.63	−0.04	0.40	4.07	−0.85	−3.32	−4.92
Atieku	3.45	1.00	1.30	3.16	4.48	1.38	0.97	0.86
Dunkwa on Offin	3.65	1.21	1.95	3.60	4.27	0.32	−0.61	−1.57
Twifo Praso	3.40	0.78	1.36	2.86	4.17	1.94	1.68	1.41
Kibi	3.92	1.00	0.83	1.43	3.87	−0.09	−1.57	−2.51
Konongo	3.89	0.91	0.76	1.53	4.43	−1.21	−3.47	−5.11
Mean	3.69	1.02	1.26	2.48	4.15	0.5	−0.62	−1.62

[a]Validated mean is the average of the models that were within an acceptable range of performance for the study area.

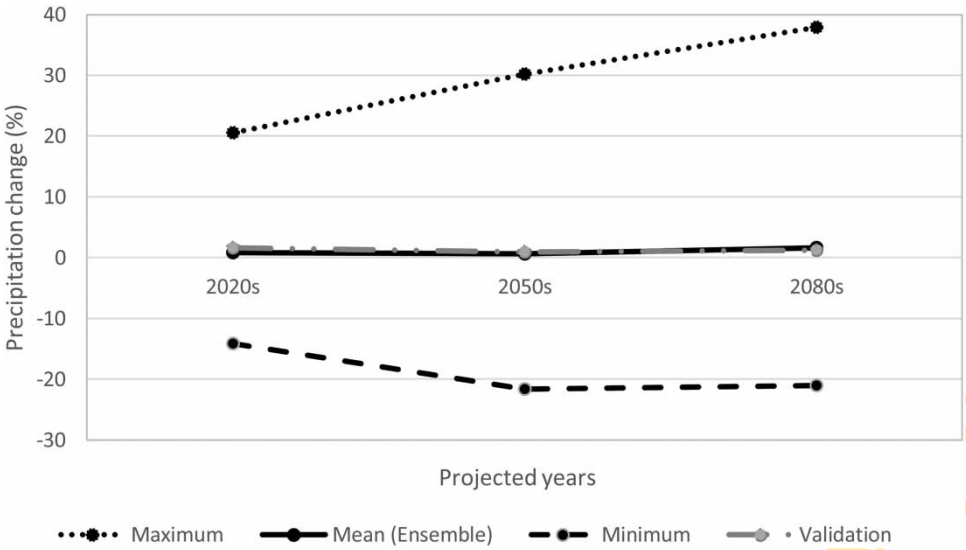

Figure 2 | Change in total rainfall projected by 43 GCMs over the Pra River Basin.

Temporal climate variability during the observed period (1981–2010)

The mean annual rainfall in the basin for the observed period was about 1446 (±226) mm with the lowest at Kumasi (1,314.66 ± 216.90) and highest at Atieku (1,553.41 ± 249.46) (Figure 3). The mean rainfall trend increased slightly at a slope of 2.78. There were seven years of drier than normal and wetter than normal in the basin from 1981 to 2010 with variability indicated by

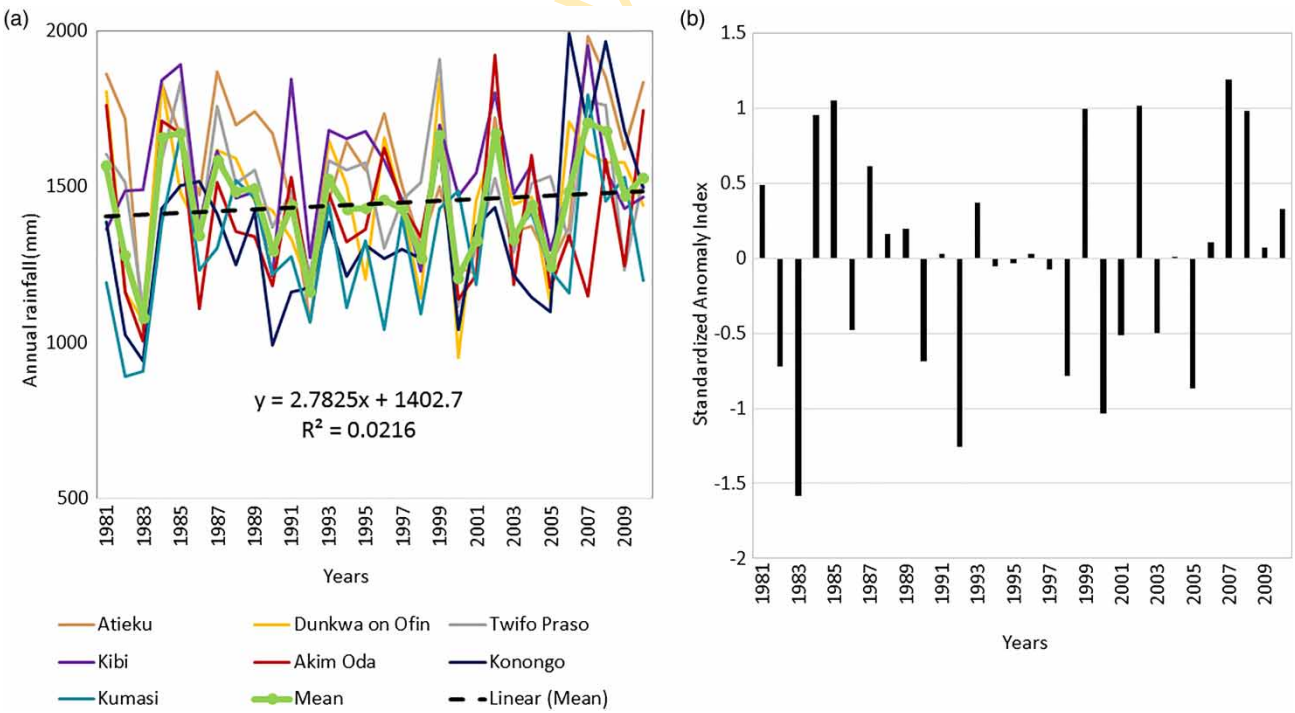

Figure 3 | Annual historical rainfall amount (mm) (a) and SAI (b) in the Pra River Basin. The linear regression model was generated by fitting a linear trend line automatically to the mean time-series graph of the seven climate stations in Microsoft Excel.

Table 5 | Performance of the models with the observed data

Models	Ateiku	Dunkwa	Twifo Praso	Kibi	Akim Oda	Konongo	Kumasi
Nash–Sutcliffe efficiency (NSE)							
CanESM	0.53	0.72	0.38	0.45[a]	0.63[a]	0.21	0.58
GFDL	0.37	0.30	0.22	0.15	0.01	0.50	0.02
Hadgem	0.53	0.75	0.51	0.418	0.71	0.70	0.50
IPSL	0.25[a]	0.06	0.35[a]	0.43[a]	0.63[a]	0.85[b]	0.02
SDSM	0.90	0.89	0.82	0.90	0.83	0.94	0.84
Root-mean-square error (RMSE)							
CanESM	0.97	0.96	1.21	1.29[a]	1.01[a]	1.48	1.10
GFDL	1.28	1.37	1.28	1.57	1.42	1.14	1.45
Hadgem	1.09	0.83	1.04	1.11	0.83	0.93	1.06
IPSL	1.47[a]	1.51	1.37[a]	1.31[a]	1.03[a]	0.64[b]	1.53
SDSM	0.53	0.58	0.71	0.54	0.67	0.43	0.69
Coefficient of determination (R^2)							
CanESM	0.72	0.85	0.66	0.98[a]	0.99[a]	0.82	0.86
GFDL	0.59	0.57	0.55	0.58	0.46	0.69	0.59
Hadgem	0.62	0.76	0.62	0.67	0.75	0.72	0.76
IPSL	0.78[a]	0.67	0.96[a]	0.96[a]	0.99[a]	0.92[b]	0.75
SDSM	0.99	0.99	0.99	0.99	0.99	0.99	0.99

[a]Linear scaling + double quantile mapping bias-corrected.
[b]Linear scaling bias-corrected.

the SAI as high as −1.59 and +1.20 in 1983 and 2007, respectively (Figure 3).

Evaluating the performance of models

Evaluating the performance of the models with the three time-series metrics showed that SDSM performed the best amongst the five models in simulating historical rainfall in the basin (Table 5). Acceptable models should have NSE values ranging between 0.0 and 1.0, lower RMSE and R^2 above 0.5 (Moriasi *et al.* 2007). Bias-corrections were applied to two stations for CanESM and to five stations for IPSL before the models fell within an acceptable range (Table 5). The WRF models (Hadgem and GFDL) at 12 km resolution needed no bias-correction to perform well. Thus, higher resolution models (SDSM and WRF) showed better agreement with the observed rainfall over the basin compared with the SMHI-RCA4 (CanESM and IPSL). Therefore, the efficiency of the models in descending order of monthly means assessment was SDSM, Hadgem, GFDL, CanESM and IPSL. The performance evaluation was done on a monthly basis since it best depicted the characteristics of change in the rainfall pattern (Gulacha & Mulungu 2016). The high variations in the performance of the models emphasised the uncertainties in climate models (Karambiri *et al.* 2011; Paeth *et al.* 2011). This could be as a result of their computational process, dynamical structure or greenhouse gas emission scenarios (Covey *et al.* 2003; Semenov & Stratonovitch 2010). It has also been found that it is more challenging to downscale precipitation compared with the temperature in Africa and this might contribute to the varying results of models on precipitation in Ghana (Hassan & Harun 2011; Obuobie *et al.* 2012; Nutsukpo *et al.* 2013).

Projected rainfall variability and change

Figure 4 shows the projected ensemble monthly mean rainfall compared with the observed records (1981–2010) and the SAI of the future period (2020–2049). In the future period from the ensemble of the five models, the mean

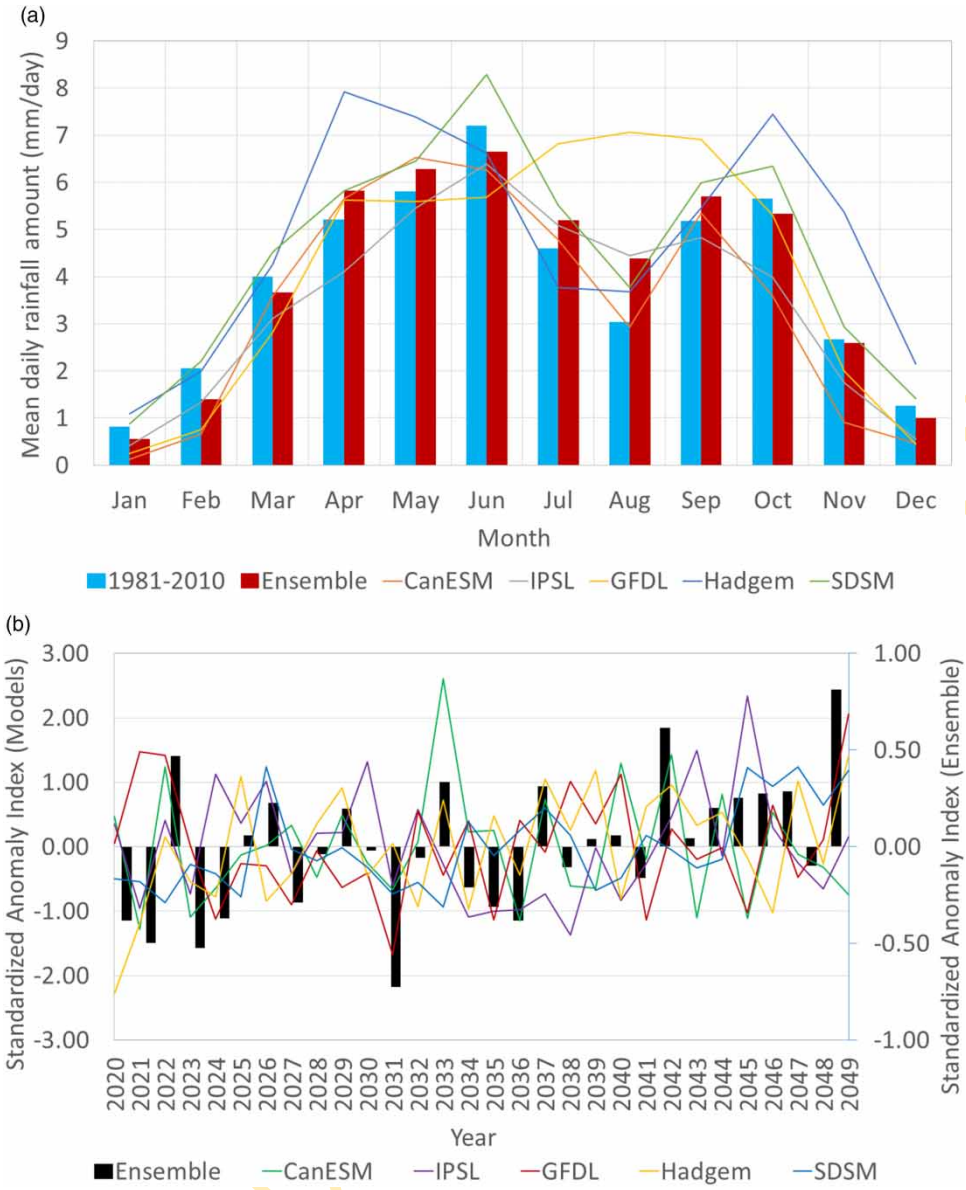

Figure 4 | Projected annual rainfall (mm) amount (a) and SAI (b) by the assessed climate models.

daily rainfall amount decreased over the basin in January, February, March, June, October, November and December at 32.14, 32.25, 8.42, 7.67, 5.72, 3.16 and 19.62%, respectively, while the remaining months experienced increases in daily rainfall amounts (Table 6). All the models succeeded in depicting the bi-modal distribution of rainfall in the basin except for GFDL, which showed a mono-modal rainfall pattern from April to October (Figure 4). The bi-modal distribution coincided with the onset of rainfall in February–March to end in August and the minor season beginning in September to end in November–December. This was similar to the results obtained by Laprise *et al.* (2013), where the ERA-driven fifth-generation Canadian Regional Climate Model was successful in reproducing the minor raining season of the Guinea Coast region in September. The increase in rainfall amount in July and August might make it seem as if there was no break from the major season into the minor season in the future period.

The SAI in Figure 4 shows that there will be drier than normal years (2021, 2023 and 2031) than wetter than

Table 6 | Rainfall percentage (%) change over the Pra River Basin (2020–2049)

Month	CanESM	IPSL	GFDL	Hadgem	SDSM	Ensemble
Jan	−85.16	−48.77	−69.13	34.80	7.56	−32.14
Feb	−67.49	−35.05	−63.05	−3.12	7.48	−32.25
Mar	−10.10	−22.14	−29.48	6.53	13.08	−8.42
Apr	8.55	−21.13	7.94	52.13	11.88	11.87
May	12.58	−5.91	−3.59	27.35	11.09	8.30
Jun	−12.93	−11.29	−21.07	−8.17	15.12	−7.67
Jul	3.87	10.65	48.20	−18.23	19.72	12.84
Aug	−3.63	46.82	132.99	21.46	24.49	44.43
Sep	3.43	−6.64	33.31	5.26	15.78	10.23
Oct	−36.53	−29.57	−6.26	31.61	12.18	−5.72
Nov	−65.91	−34.80	−25.35	100.81	9.46	−3.16
Dec	−63.08	−55.47	−64.27	71.49	13.25	−19.62
Mean	−26.37	−17.78	−4.98	26.83	13.43	−1.77

normal years (2042 and 2049) during 2020–2049. However, 2020 (−0.38) and 2036 (−0.38) are closer to drier than normal years and should be considered in planning against drought with the three projected years with SAI < −0.5. Hadgem and CanESM recorded the highest negative (−2.28) and positive (2.61) SAI in the year 2020 and 2033, respectively. The CanESM and IPSL projections (Table 6) with a respective 26% and 18% decrease in rainfall are similar to the findings of Obuobie *et al.* (2012), where an ECHAM4/CSIRO joint model showed rainfall decreases of 17.8% by 2020 and 25.9% by 2050. This could be attributed to the similarities in their spatial resolution (44–55 km). However, SDSM (best model) and Hadgem (second best model) projected rainfall increase of 13.4% and 26.8%, respectively, with GFDL (third best model) projecting a decrease of 4.9%. The projected increase of rainfall by the two best models in this study is in agreement with the findings of Donat *et al.* (2014) who project that the world's dry places like the tropics will experience more extreme precipitation, which could result in rainfall increase. The dry seasons of the bi-modal rainfall patterns in the basin were during July–August and November–March (Dickson & Benneh 1995). The ensemble results show that the future rainfall pattern in the basin could favour the short dry season between July and August because rainfall is projected to increase by 12.8% and 44.4%, respectively (Table 6). The advantages of these findings are that crops requiring a constant supply of water for maturing may receive enough water from April to September (HarvestChoice 2010; Guan *et al.* 2015). Consequently, the harvest period of cash crops like cocoa may increase, thereby increasing farmers' yields (HarvestChoice 2010; Preethi & Revadekar 2013). Disadvantages of the projected increase in monthly rainfall (Table 6) include the rise in vector-borne diseases such as malaria and dengue fever as breeding grounds increase (Githeko *et al.* 2000; Thomson *et al.* 2018) and the possibility of floods (Colwell *et al.* 2008). However, the major dry season (November–March) may be elongated by the future rainfall decrease from October to March with increased dry spells between December and January at a mean rate of 28% (Figure 4, Table 6). The disadvantages will range from rise in the occurrence of bush fire (Drever *et al.* 2009; Xystrakis *et al.* 2014), increased herdsman–farmer conflicts as they compete for farmland with foliage for their flocks (Kima *et al.* 2016; Bessah *et al.* 2019) and food insecurity (Blanc 2012; Guan *et al.* 2015; Fishman 2016).

The spatial distribution of the projected rate of change (%) in the mean annual rainfall amount from 2020 to 2049 varied amongst the models as shown in Figure 5. The SDSM and Hadgem had similar spatial rainfall distributions of increasing amounts southward and at the east end of the basin. The SDSM and Hadgem projected a rate of change between 8–19% and 0–29%, respectively. The GFDL also projected an increasing trend in the southern part of the

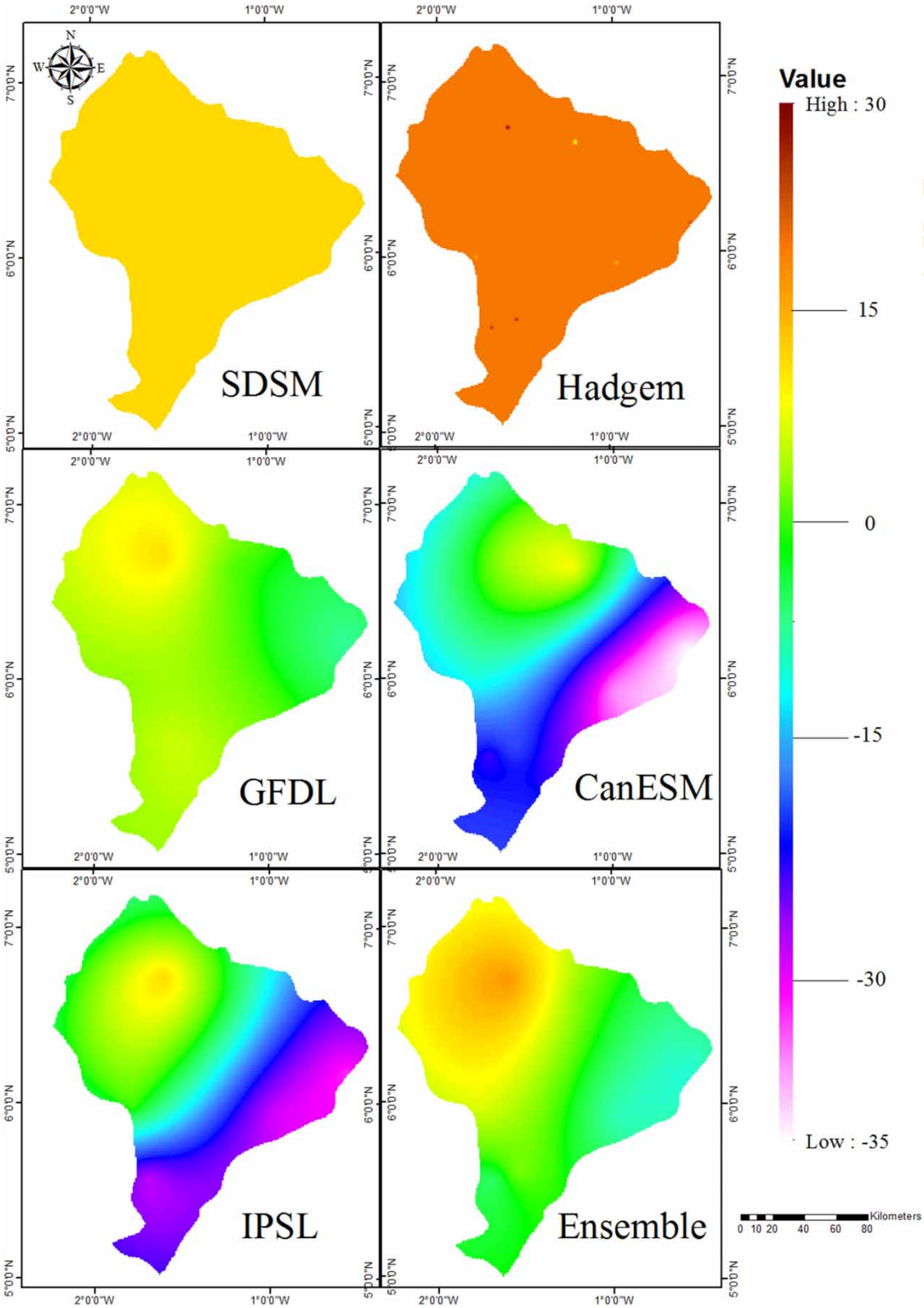

Figure 5 | The projected rate of change (%) in the mean annual rainfall by models (2020–2049).

basin, which has forest cover and coastal savannah zones of about 3–5% and in the north (2–17%). The rate of change by GFDL from the centre to the east of the basin was uniform (Figure 5). The CanESM and IPSL models projected that rainfall would increase spatially northward in the basin, that is, increasing rainfall in the semi-deciduous zones, while the forest and coastal savannah zones have a decreasing amount of rainfall between 1% and 35%. This might result in an increased runoff in the deciduous zones leading to flooding. The ensemble captured spatial increasing rate of change in the mean annual rainfall amount from the east to the west in the range of 4–8%. The ensemble suggests a decrease in rainfall at the east end of the basin. Adaptation measures need to be assessed to prevent shocks from the projected changes if it happens.

Variations in onset, cessation and duration of rainfall

Figure 6 presents the rainfall onset, cessation dates and the LRS projected by the five models and the reference records of the observed period (1981–2010). During the observed period, early onset rainfall was on 4th February 2004 and the late-onset was on 6th April 1983. Early and late cessation dates were on 16th October 1987 and 15th December 1990, respectively, with an average LRS at 255 days. The rainy season is defined as the period where the total monthly rainfall was equal to or above 50.8 mm (Matthew *et al.* 2017). There was a drought in the year 1983 in Ghana, as rainfall ceased on 26th October, giving the lowest span of rainy days (218 days) during the 30-year observed period (1981–2010). The rainfall onset had a decreasing trend, that is, onset became earlier over the observed period and increasingly had a later cessation date. This implied that the LRS increased across the years over the basin in the observed period, starting with 243 days in 1981 and increasing to 289 days in 2010 (Figure 6). The method does not account for the break in the bi-modal rainfall pattern in the semi-deciduous forest zone, which occurs in July and August before the minor rains start in September (Dickson & Benneh 1995).

The SDSM and Hadgem models projected an average LRS of 267 and 278 days, respectively, in the period 2020–2049. There is a projection of increased rainy days by 12 and 23 days from the observed period, whereas GFDL, CanESM and IPSL projected a decrease in rainy days by 29, 40 and 33 days, respectively. Rainfall onset, as projected by SDSM, from 2020 to 2049 will be as early as 5th February in 2045 and lightly later on 13th March in 2039. Cessation is on 22nd October 2034 and 17th December 2026 for early and late cessation, respectively (Figure 6). Hadgem, on the other hand, projected an early onset on 31st January 2027 and the late-onset on 28th March 2021, while the early and late rainfall cessation was on 4th November 2028 and 20th December 2038, respectively (Figure 6). According to the best performing models from this study, it implies that rainfall onset will be delayed by one month from the observed period into the future period, while rainfall cessation will be maintained in the same months with additional rainy days before ending.

The GFDL projected early and late-onset of rainfall in February and April and rainfall cessation to be October and November with 225 days as the rainy season. The GFDL projected increasing trends for both onset and cessation of rainfall, which implies that rainfall will start late and end early in 2020–2049. There was a slight difference between the projection of the GFDL, CanESM and IPSL models. The CanESM and IPSL (SMHI-RCA4) models showed decreasing trends in rainfall onset and cessation. It implies that rainfall onset is expected to be late and cessation to be early across future periods. The average LRS for CanESM and IPSL were 215 and 222 days, respectively. Early and late-onset for SMHI-RCA4 models were in February and April, respectively, while early cessation was in September and October for CanESM and IPLS, respectively. Late rainfall cessation for SMHI-RCA4 models was projected to be in November. The GFDL and Hadgem models, which have the same spatial resolution running on the WRF model, performed differently in this study. This might be due to the varying boundary conditions under which the RCMs were set in the GCMs (Nikiema *et al.* 2016).

Table 7 presents the onset date, cessation date and LRS at the seven stations considered in the study. The observed period was between 1981 and 2010, whereas the projected years were between 2020 and 2049. Two synoptic stations, namely Akim Oda and Kumasi, were used as references, based on findings from other studies. At the Akim Oda station, early and late-onset of rainfall was on 23rd January

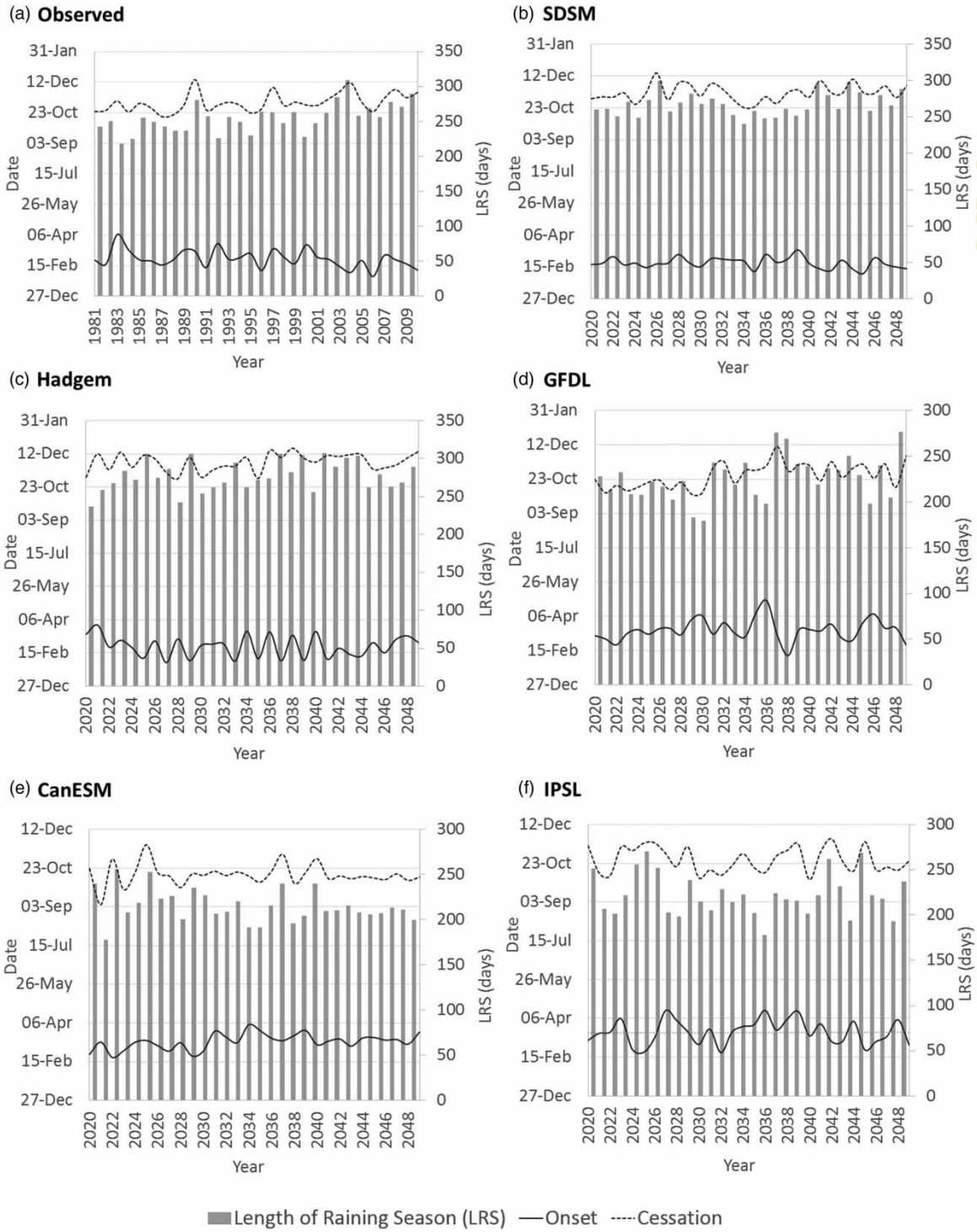

Figure 6 | Observed and projected rainfall onset, rainfall cessation and length of raining season over the Pra River Basin.

and 4th April, respectively, while early and late cessation of rainfall was on 3rd October and 25th December, respectively. The mean onset and cessation dates for the observed period were on 27th February and 18th November, respectively. The average LRS was 264 (±30) days. Mensah *et al.* (2016) used the fuzzy logic approach in Instat software to

Table 7 | Onset, cessation and LRS of the observed (1981–2010) and model projections (2020–2049) at the selected stations in the Pra River Basin

	Onset of rainfall				Cessation of rainfall				
Data	**Early**	**Late**	**Mean**	**SD (days)**	**Early**	**Late**	**Mean**	**SD (days)**	**LRS (days)**
Akim Oda Station									
Observed	23 Jan	04 Apr	27 Feb	20	03 Oct	25 Dec	18 Nov	23	264 (± 30)
SDSM	21 Jan	16 Mar	20 Feb	14	03 Oct	31 Dec	24 Nov	26	277 (± 30)
Hadgem	22 Jan	01 Apr	23 Feb	18	01 Nov	31 Dec	30 Nov	23	280 (± 29)
GFDL	11 Feb	01 May	16 Mar	20	01 Oct	20 Dec	27 Oct	23	225 (± 30)
CanESM	3 Feb	10 May	19 Mar	24	01 Sept	31 Dec	26 Oct	33	221 (± 46)
IPSL	1 Feb	03 Jun	31 Mar	35	01 Oct	29 Dec	10 Nov	27	224 (± 48)
Ateiku Station									
Observed	11 Jan	14 Apr	21 Feb	20	15 Sept	29 Dec	16 Nov	28	268 (± 34)
SDSM	05 Feb	01 Apr	25 Feb	13	01 Oct	29 Dec	18 Nov	23	266 (± 26)
Hadgem	13 Jan	04 Apr	09 Feb	22	01 Nov	30 Dec	09 Dec	17	303 (± 29)
GFDL	19 Jan	10 Apr	08 Mar	22	01 Oct	30 Dec	10 Nov	28	248 (± 38)
CanESM	02 Feb	05 Apr	10 Mar	12	04 Sept	22 Nov	12 Oct	19	215 (± 22)
IPSL	18 Jan	17 Apr	06 Mar	21	01 Sept	23 Dec	06 Nov	28	246 (± 35)
Dunkwa on Ofin Station									
Observed	21 Jan	05 Apr	26 Feb	16	01 Oct	24 Dec	09 Nov	28	256 (± 32)
SDSM	23 Jan	05 Apr	26 Feb	17	01 Oct	28 Dec	22 Nov	26	268 (± 31)
Hadgem	22 Jan	02 Apr	22 Feb	18	02 Nov	31 Dec	04 Dec	23	285 (± 26)
GFDL	19 Jan	10 Apr	15 Mar	21	01 Oct	28 Dec	01 Nov	27	231 (± 31)
CanESM	26 Feb	04 Apr	13 Mar	10	03 Sept	22 Nov	14 Oct	16	215 (± 21)
IPSL	17 Feb	10 Apr	18 Mar	13	01 Oct	30 Nov	21 Oct	22	217 (± 29)
Kibi Station									
Observed	11 Jan	20 Apr	21 Feb	20	01 Oct	30 Dec	17 Nov	29	269 (± 35)
SDSM	15 Jan	05 Mar	03 Feb	13	01 Oct	27 Dec	29 Nov	30	299 (± 35)
Hadgem	02 Feb	03 Apr	27 Feb	20	01 Nov	23 Dec	28 Nov	21	274 (± 31)
GFDL	14 Feb	23 Apr	20 Mar	18	24 Aug	30 Dec	26 Oct	30	220 (± 27)
CanESM	15 Jan	03 May	09 Mar	18	15 Sept	10 Dec	15 Oct	24	220 (± 31)
IPSL	05 Jan	01 Jun	16 Mar	31	03 Sept	29 Dec	29 Oct	28	226 (± 40)
Konongo Station									
Observed	28 Jan	02 May	02 Mar	21	04 Sept	23 Dec	22 Oct	25	235 (± 32)
SDSM	02 Feb	06 Apr	22 Feb	21	01 Oct	28 Dec	25 Oct	29	241 (± 39)
Hadgem	07 Feb	07 Apr	12 Mar	17	01 Oct	31 Dec	12 Nov	23	246 (± 25)
GFDL	05 Mar	24 Apr	25 Mar	14	01 Oct	29 Nov	19 Oct	20	208 (± 25)
CanESM	27 Feb	03 Apr	14 Mar	9	04 Sept	15 Nov	11 Oct	13	211 (± 15)
IPSL	12 Jan	13 Apr	09 Mar	23	04 Oct	31 Dec	28 Oct	26	233 (± 36)
Kumasi Station									
Observed	14 Jan	02 Apr	27 Feb	17	01 Oct	21 Dec	22 Oct	26	237 (± 32)
SDSM	01 Feb	10 Mar	27 Feb	15	01 Oct	24 Dec	21 Oct	24	236 (± 29)

(*continued*)

Table 7 | continued

	Onset of rainfall				Cessation of rainfall				
Data	**Early**	**Late**	**Mean**	**SD (days)**	**Early**	**Late**	**Mean**	**SD (days)**	**LRS (days)**
Hadgem	04 Feb	05 Apr	09 Mar	17	01 Oct	31 Dec	21 Nov	24	257 (± 31)
GFDL	26 Jan	20 Apr	02 May	19	01 Oct	23 Dec	20 Oct	22	211 (± 32)
CanESM	25 Feb	04 Apr	13 Mar	09	02 Sept	15 Nov	11 Oct	14	212 (± 15)
IPSL	22 Feb	09 Apr	19 Mar	12	01 Oct	21 Nov	12 Oct	14	207 (± 21)
Twifo Praso Station									
Observed	17 Jan	08 Apr	28 Feb	25	01 Oct	29 Dec	12 Nov	25	257 (± 35)
SDSM	23 Jan	01 Apr	18 Feb	17	01 Nov	30 Dec	28 Nov	25	283 (± 28)
Hadgem	14 Jan	04 Apr	12 Feb	21	01 Nov	26 Dec	09 Dec	17	300 (± 27)
GFDL	08 Feb	05 Apr	08 Mar	20	01 Oct	22 Dec	03 Nov	25	240 (± 37)
CanESM	21 Feb	05 Apr	12 Mar	10	04 Sept	26 Nov	12 Oct	19	213 (± 22)
IPSL	11 Mar	14 May	01 Apr	15	01 Sept	28 Nov	21 Oct	25	203 (± 27)

LRS – length of raining season.

determine the onset date, cessation date and length of raining season for Akim Oda for the period 1998–2012. The mean onset and cessation dates were on 15th March and 10th November, respectively, and the duration was 240 days (Mensah *et al.* 2016). Amekudzi *et al.* (2015) used the percentage mean cumulative rainfall method over the period 1970–2012 and to determine the onset dates, cessation dates and length of rain to be 11th March, 6th/11th November (rainfall amount/rainy days) and 245 days, respectively. Comparatively, the study's modified Walter–Olaniran method (Matthew *et al.* 2017) results were 7 and 19 days over that of cumulative curves method of Amekudzi *et al.* (2015) for cessation date and LRS, respectively, and 8 days for cessation date and 24 days for LRS above the results of Mensah *et al.* (2016). However, the mean onset date was earlier in this study at 12 and 16 days before the determined onset by Amekudzi *et al.* (2015) and Mensah *et al.* (2016), respectively.

At the Kumasi station, early and late-onset of rainfall was on 14th January and 2nd April, respectively, while early and late cessation of rainfall was on 1st October and 21st December, respectively. The mean onset and cessation dates for the observed period were on 27th February and 22nd October, respectively. The average LRS was 237 (±32) days (Table 7). Amekudzi *et al.* (2015) determined the onset, cessation and LRS for the Kumasi station to be 11th March, 22nd/27th October (rainfall amount/rainy days) and 300 days, respectively. Cessation dates of this study were the same when using the method of rainfall amount to determine the cessation date of Amekudzi *et al.* (2015), although the period of analysis was 30 and 43 years, respectively. Onset was earlier in this study when compared with that of Amekudzi *et al.* (2015). Mensah *et al.* (2016) also determined 21st March, 20th November and 244 days as the onset, cessation and LRS for the Kumasi station between 1998 and 2012. The difference in onset and cessation dates of the two methods compared with the method of this study was less than 15 days. A study with the same period is hereby recommended to test the modified method of this study with other available methods to determine its efficiency. The mean observed onset at all stations in this study was in February, except the Konongo station, which was in March (Table 7). November was the month for the mean observed cessation date at all stations, except at Kumasi and Konongo, which was in October.

On average at all stations, SDSM and Hadgem projected the mean onset date earlier than what was determined for the observed period or the same month, while GFDL, CanESM and IPSL projected the late-onset of rainfall in relation to the observed period. However, at Kibi, Konongo and Kumasi, the future onset date of Hadgem was about

5 days later than the observed period. The trend was the same with projected cessation dates by all models. On average SDSM and Hadgem projected the late cessation dates compared with the observed period, whereas GFDL, CanESM and IPSL projected an early cessation.

The projected LRS increased with SDSM and Hadgem, whereas GFDL, CanESM and IPSL projected a decrease in the length of the rainy days. The projected increased length of the rainy days will facilitate crop growth since growth depends more on the number of rainy days in the season than the amount (Lebel & Le Barbe 1997; Vischel & Lebel 2007). In addition, the hydrological cycle will be positively affected by the projection of SDSM and Hadgem (Modarres 2010). However, the decreased LRS projected by GFDL, CanESM and IPSL might result in prolonged drought and stunted crop growth.

CONCLUSIONS

The study established that the performance of the models based on the agreement of their historical simulations with station records using time-series metrics analyses in descending order was SDSM, Hadgem, GFDL, CanESM and IPSL. Based on the results of the models with the best ability (SDSM and Hadgem), the rainfall amount is projected to increase in the basin. This is contrary to findings of early research in the basin using low to medium resolution climate models (CanESM and IPSL). However, the ensemble projection of below 2% decrease in the rainfall amount fits into the findings of AR4 climate change scenarios over the West African sub-region and the IPCC Fifth Assessment report 43 GCMs projections over the Pra River Basin. The ensemble monthly projections indicate that the minor dry season (July–August) could have enough rain to change the rainfall pattern to follow a mono-modal type from April to September and a long dry spell from October to March. There could be a severe water scarcity according to the projection of the ensemble. The SAI results of the likelihood of drier than normal years further confirm the findings on a monthly variation in rainfall, which might result in drought. The modified approach in determining the rainfall onset, cessation and duration was closely related to other existing methods and will, therefore, need further modification to capture the bi-modal trend in rainfall in the basin. According to SDSM and Hadgem models, the rainfall onset date and cessation date are projected to be earlier and later, which consequently increases the rainy days without capturing the short dry season before the minor rainy season starts. The increase in the LRS might lead to more flooding or short dry spells within a season, depending on the distribution and intensity of rainfall. The study has shown that high-resolution models are better equipped to simulate rainfall at the basin or point scale. Thus, high-resolution models should be combined with other mid-resolution models in projecting rainfall to determine the climate change impact, vulnerability, adaptation planning and policy formulations. Alternative sources of water should be sought to supplement rainfed crop production considering the dry spell projection of the ensemble. This will have an impact on food security since the basin contributes highly to the production of cash crops like cocoa and tuber crops with valuable economic gains to the nation.

ACKNOWLEDGEMENTS

This study formed part of a PhD research under the Pan African University Institute of Life and Earth Sciences at the University of Ibadan (Nigeria), funded by the African Union Commission. The authors acknowledge the Ghana Meteorological Agency for the rainfall data. The authors thank the University of Prince Edward Island (UPEI) for granting access to their climate database for 43 GCMs analysis. The authors are also grateful to CORDEX Africa-domain for accessing SMHI-RCA4 models at climate4impact.eu and West Africa Science Service Center on Climate Change and Adapted Land Use (WASCAL) Geoportal, for WRF model downloads. Finally, the authors are grateful to co-public.lboro.ac.uk for giving free access to the SDSM model and NCEP data.

REFERENCES

Aguilar, E., Aziz Barry, A., Brunet, M., Ekang, L., Fernandes, A., Massoukina, M., Mbah, J., Mhanda, A., do Nascimento, D. J., Peterson, T. C., Thamba Umba, O., Tomou, M. & Zhang, X.

2009 Changes in temperature and precipitation extremes in western central Africa, Guinea Conakry, and Zimbabwe, 1955–2006. *Journal of Geophysical Research* **114**, 1–11.

Ahiataku-Togobo, W. 2014 Renewable energy in Ghana: policy and potential. In: *Presented at UNEF Spanish Solar Forum*, 18–19 November, Madrid, Spain.

Ambrosino, C. 2011 *Rainfall Variability in Southern Africa: Drivers, Climate Changes and Implication for Agriculture*. Doctoral Thesis, University College London (UCL).

Amekudzi, L. K., Yamba, E. I., Preko, K., Asare, E. O., Aryee, J., Baidu, M. & Codjoe, S. N. A. 2015 Variabilities in rainfall onset, cessation and length of rainy season for the various agro-ecological Zones of Ghana. *Climate* **3**, 416–434. doi:10.3390/cli3020416.

Arguez, A., Durre, I., Applequist, S., Vose, R. S., Squires, M. F., Yin, X., Heim Jr., R. R. & Owen, T. W. 2012 NOAA'S 1981–2010 U.S. climate normals: An overview. *Bulletin of American Meteorological Society* **93**, 1687–1697. doi:10.1175/BAMS-D-11-00197.1.

Bessah, E., Raji, A. O., Taiwo, O. J., Agodzo, S. K. & Ololade, O. O. 2018 Variable resolution modeling of near future mean temperature changes in the dry sub-humid region of Ghana. *Modeling Earth Systems and Environment* **4** (3), 919–933. doi:10.1007/s40808-018-0479-0.

Bessah, E., Bala, A., Agodzo, S. K., Okhimamhe, A. A., Boakye, E. A. & Ibrahim, S. U. 2019 The impact of crop farmers' decisions on future land-use land-cover changes in Kintampo north municipality of Ghana. *International Journal of Climate Change Strategies and Management* **11** (1), 72–87. doi:10.1108/IJCCSM-05-2017-0114.

Blanc, E. 2012 The impact of climate change on crop yields in Sub-Saharan Africa. *American Journal of Climate Change* **1** (1), 1–13. doi:10.4236/ajcc.2012.11001.

Bo, L., Erika, S. S., Ian, B., Elizabeth, M. & Saleemul, H. 2004 *Adaptation Policy Frameworks for Climate Change. Developing Strategies, Policies and Measures*. Cambridge University Press, Cambridge.

Boon, E. & Ahenkan, A. 2012 Assessing climate change impacts on ecosystem services and livelihoods in Ghana: case study of communities around Sui Forest Reserve. *Journal of Ecosystem and Ecography* **S3**, 1–8. doi:10.4172/2157-7625.S3-001.

Brahic, C. 2007 The impacts of rising global temperatures. Available from: https://www.newscientist.com/article/dn11089-the-impacts-of-rising-global-temperatures/ (accessed 8 January 2018)

Burke, M. B., Miguel, E., Satyanath, S., Dykema, J. A. & Lobell, D. B. 2009 Warming increases the risk of civil war in Africa. *Proceedings of National Academy of Science* **106**, 20670–20674.

Canon, A. J., Sobie, S. R. & Murdock, T. Q. 2015 Bias correction of GCM precipitation by quantile mapping: how well do methods preserve changes in quantiles and extremes? *Journal of Climate* **28**, 6938–6959. doi:10.1175/JCLI-D-14-00754.1.

Chylek, P., Li, J., Dubey, M. K., Wang, M. & Lesins, G. 2011 Observed and model simulated 20th century Arctic temperature variability: Canadian earth system model CanESM2. *Atmospheric Chemistry and Physics Discussion* **11**, 22893–22907. doi:10.5194/acpd-11-22893-2011.

Colwell, R. K., Brehm, G., Cardelús, C., Gilman, A. C. & Longino, J. T. 2008 Global warming, elevational range shifts, and lowland biotic attrition in the wet tropics. *Science* **322**, 258–261.

Covey, C., Achuta-Rao, K. M., Cubasch, U., Jones, P., Lambert, S. J., Mann, M. E., Phillips, T. J. & Taylor, K. E. 2003 An overview of results from the coupled model inter comparison project. *Global Planet Change* **37** (1), 103–133. doi:10.1016/S0921-8181(02)00193-5.

Cubasch, U., Wuebbles, D., Chen, D., Facchini, M. C., Frame, D., Mahowald, N. & Winther, J.-G. 2013 Introduction. In: *Climate Change 2013: The Physical Science Basis. Contribution of Working Group I to the Fifth Assessment Report of the Intergovernmental Panel on Climate Change* (T. F. Stocker, D. Qin, G.-K. Plattner, M. Tignor, S. K. Allen, J. Boschung, A. Nauels, Y. Xia, V. Bex & P. M. Midgley, eds). Cambridge University Press, Cambridge, pp. 119–158.

Davis, J., O'Grady, A. P., Dale, A., Arthington, A. H., Gell, P. A., Driver, P. D., Bond, N., Casanova, M., Finlayson, M., Watts, R. J., Capond, S. J., Nagelkerken, I., Tingley, R., Fry, B., Page, T. J. & Specht, A. 2015 When trends intersect: the challenge of protecting freshwater ecosystems under multiple land use and hydrological intensification scenarios. *Science of the Total Environment* **534**, 65–78.

Déandreis, C., Pagé, C., Braconnot, P., Bärring, L., Bucchignani, E., de Cerff W., S., Hutjes, R., Joussaume, S., Mares, C., Planton, S. & Plieger, M. 2014 Towards a dedicated impact portal to bridge the gap between the impact and climate communities: lessons from use cases. *Climatic Change* **125**, 333–347. doi:10.1007/s10584-014-1139-7.

Dickson, K. B. & Benneh, G. 1995 *A New Geography of Ghana*, 3rd edn. Longman Book Company, London.

Diffenbaugh, N. S. & Giorgi, F. 2012 Climate change hotspots in the CMIP5 global climate model ensemble. *Climatic Change* **114** (3–4), 813–822.

Donat, M. G., Peterson, T. C., Brunet, M., King, A. D., Almazroui, M., Kolli, R. K., Boucherf, D., Al-Mulla, A. Y., Nour, A. Y., Aly, A. A., Nada, T. A. A., Semawi, M. M., Al Dashti, H. A., Salhab, T. G., El Fadli, K. I., Muftah, M. K., Eida, S. D., Badi, W., Driouech, F., El Rhaz, K., Abubaker, M. J. Y., Ghulam, A. S., Erayah, A. S., Mansour, M. B., Alabdouli, W. O., Al Dhanhani, J. S. & Al Shekaili, M. N. 2014 Changes in extreme temperature and precipitation in the Arab region: Long-term trends and variability related to ENSO and NAO. *International Journal of Climatology* **34**, 581–592. doi:10.1002/joc.3707.

Dosio, A. & Panitz, H.-J. 2016 Climate change projections for CORDEX–Africa with COSMO–CLM regional climate model and differences with the driving global climate models. *Climate Dynamics* **46**, 1599–1625. doi:10.1007/s00382-015-2664-4.

Drever, C. R., Bergeron, Y., Drever, M. C., Flannigan, M., Logan, T. & Messier, C. 2009 Effects of climate on occurrence and

size of large fires in a northern hardwood landscape: historical trends, forecasts, and implications for climate change in Témiscamingue, Québec. *Applied Vegetation Science* **12** (3), 261–272.

FAO 2009 *Climate Change Adaptation*. Food and Agricultural Organization (FAO), Rome, pp. 1–19.

Fenech, A., Comer, N. & Gough, W. 2007 Selecting a global climate model for understanding future scenarios of climate change. In: *Linking Climate Models to Policy and Decision-Making* (A. Fenech & J. MacLellan, eds). Environment Canada, Toronto, Ontario, Canada, pp. 133–145.

Fishman, R. 2016 More uneven distributions overturn benefits of higher precipitation for crop yields. *Environmental Research Letters* **11**, 024004. doi:10.1088/1748-9326/11/2/024004.

Garbutt, D. J., Stern, R. D., Denett, M. D. & Elston, J. 1981 A comparison of the rainfall climate of eleven places in West Africa, using a two-part model for daily rainfall. *Archives for Meteorology, Geophysics, and Bioclimatology* **29**, 137–155.

Giorgi, F., Jones, C. & Asrar, G. R. 2009 Addressing climate information needs at the regional level: the CORDEX framework. *World Meteorological Organization Bulletin* **58** (3), 175–183.

Githeko, A. K., Lindsay, S. W., Confalonieri, U. E. & Patz, J. A. 2000 Climate change and vector-borne diseases: a regional analysis. *Bulletin of the World Health Organization* **78** (9), 1136–1147.

Goodess, C., Anagnostopoulou, C., Bárdossy, A., Frei, C., Harpham, C., Haylock, M. R., Hundecha, Y., Maheras, P., Ribalaygua, J., Schmidli, J., Schmith, T., Tolika, K., Tomozeiu, R. & Wilby, R. L. 2011 An intercomparison of statistical downscaling methods for Europe and European regions – assessing their performance with respect to extreme temperature and precipitation events. *Climatic Research Unit Research Publication* **11**, 1–68.

Guan, K., Sultan, B., Biasutti, M., Baron, C. & Lobell, D. B. 2015 What aspects of future rainfall changes matter for crop yields in West Africa? *Geophysical Research Letters* **42**, 8001–8010. doi:10.1002/ 2015GL063877.

Gulacha, M. M. & Mulungu, D. M. M. 2016 Generation of climate change scenarios for precipitation and temperature at local scales using SDSM in Wami-Ruvu River Basin Tanzania. *Physics and Chemistry of the Earth* 1–11. doi:10.1016/j.pce.2016.10.003.

Hadgu, G., Tesfaye, K., Mamo, G. & Kassa, B. 2013 Trend and variability of rainfall in Tigray, Northern Ethiopia: analysis of meteorological data and farmers' perception. *Academia Journal of Agricultural Research* **1** (6), 88–100. doi:10.15413/ajar.2013.0117.

HarvestChoice 2010 *Rainfall Variability and Crop Yield Potential*. International Food Policy Research Institute, Washington, DC. Available from: http://harvestchoice.org/node/2240 (accessed 3 March 2019).

Hassan, Z. & Harun, S. 2011 Statistical downscaling for climate change scenarios of rainfall and temperature. In: *Presented at United Kingdom-Malaysia-Ireland Engineering Science Conference (UMIES)*, Malaysia.

Hatfield, J. L. & Prueger, J. H. 2015 Temperature extremes: effect on plant growth and development. *Weather and Climate Extremes* **10**, 4–10.

Heinzeller, D. 2019 *WASCAL – Regional Climate Simulations for West Africa*. Available from: https://www.dkrz.de/projects-and-partners/projects/focus/wascal-en (accessed 3 March 2019)

Heinzeller, D., Olusegun, C. & Kunstmann, H. 2016a *High Resolution (12 km) WRF-GFDL Daily Outputs of Simulated Near-Surface Air Temperature over West Africa, 1980–2009 (WASCAL Project)*. Available from: https://wascal-dataportal.org/geonetwork/?uuid=cbcbda5f-7dda-4764-8783-e022a58e2885 (accessed 25 June 2017).

Heinzeller, D., Olusegun, C. & Kunstmann, H. 2016b *High Resolution (12 km) WRF-HADGEM2 Daily Outputs of Simulated Precipitation over West Africa, 1980 - 2009 (WASCAL Project)*. Available from: https://wascal-dataportal.org/geonetwork/apps/search/?uuid=a972e985-93dd-4f84-9f24-a57f94a58d0d (accessed 25 June 2017).

IPCC 2007 Summary for policymakers. In: *Climate Change 2007: The Physical Science Basis. Contribution of Working Group I to the Fourth Assessment Report of the Intergovernmental Panel on Climate Change* (S. Solomon, D. Qin, M. Manning, Z. Chen, M. Marquis, K. B. Averyt, M. Tignor & H. L. Miller, eds). Cambridge University Press, Cambridge, pp. 1–18.

IPCC 2014 *Climate Change 2014: Synthesis Report. Contribution of Working Groups I, II and III to the Fifth Assessment Report of the Intergovernmental Panel on Climate Change* (Core Writing Team, R. K. Pachauri & L. A. Meyer, eds). IPCC, Geneva, Switzerland, p. 151.

Karambiri, H., Garcı´a Galiano, S., Giraldo, J., Yacouba, H., Ibrahim, B., Barbier, B. & Polcher, J. 2011 Assessing the impact of climate variability and climate change on runoff in West Africa: the case of Senegal and Nakambe River basins. *Atmospheric Science Letters* **12** (1), 109–115. doi:10.1002/asl.317.

Kima, S. A., Okhimamhe, A. A. & Kiema, A. 2016 Assessing the impacts of land use and land cover change on pastoral livestock farming in South-Eastern Burkina Faso. *Environment and Natural Resources Research* **6** (1), 110–124. doi:10.5539/enrr.v6n1p110.

Knox, J. W., Hess, T. M., Daccache, A. & Perez Ortola, M. 2013 *What Are the Projected Impacts of Climate Change on Food Crop Productivity in Africa and South Asia?* Available from: http://r4d.dfid.gov.uk/Output/186428/ (accessed 28 March 2019).

Kusimi, J. M., Yiran, G. A. B. & Attua, E. M. 2015 Soil erosion and sediment yield modelling in the Pra River Basin of Ghana using the Revised Universal Soil Loss Equation (RUSLE). *Ghana Journal of Geography* **7** (2), 38–57.

Laprise, R., Hernández-Díaz, L., Tete, K., Sushama, L., Šeparović, L., Martynov, A., Winger, K. & Valin, M. 2013 Climate projections over CORDEX Africa domain using the fifth-generation

Canadian Regional Climate Model (CRCM5). *Climate Dynamics* **41**, 3219–3246. doi:10.1007/s00382-012-1651-2.

Lebel, T. & Le Barbe, L. 1997 Rainfall monitoring during HAPEX-Sahel. 2. Point and areal estimation at the event and seasonal scales. *Journal of Hydrology* **188**, 97–122. doi:10.1016/S0022-1694(96)03325-2.

Lenderink, G., Buishand, A. & Van Deursen, W. 2007 Estimates of future discharges of the river Rhine using two scenario methodologies: direct versus delta approach. *Hydrology and Earth System Science* **11** (3), 1145–1159.

Lomborg, B. 2016 Impact of current climate proposals. *Global Policy* **7** (1), 109–118.

López-Moreno, J. I., Vicente-Serrano, S. M., Moran-Tejeda, E., Zabalza, J., Lorenzo-Lacruz, J. & García-Ruiz, J. M. 2011 Impact of climate evolution and land use changes on water yield in the Ebro basin. *Hydrology and Earth System Science* **15**, 311–322.

Marcé, R., Rodríguez-Arias, M. A., García, J. C. & Armengol, J. 2010 El Niño southern oscillation and climate trends impact reservoir water quality. *Global Change Biology* **16**, 2857–2865.

Matthew, O. J., Imasogie, O. G., Ayoola, M. A., Abiye, O. E. & Sunmonu, L. A. 2017 Assessment of prediction schemes for estimating rainfall onset over different climatic zones in West Africa. *Journal of Geography, Environment and Earth Science International* **9** (1), 1–15.

Mawunya, F. D., Adiku, S. G. K., Laryea, K. B., Yangyuoru, M. & Atika, E. 2011 Characterisation of seasonal rainfall for cropping schedules. *West African Journal of Applied Ecology* **19**, 107–118.

Mensah, C., Amekudzi, L. K., Klutse, N. A. B., Aryee, J. N. A. & Asare, K. 2016 Comparison of rainy season onset, cessation and duration for Ghana from RegCM4 and GMet datasets. *Atmospheric and Climate Sciences* **6**, 300–309.

Modarres, R. 2010 Regional dry spells frequency analysis by l-moment and multivariate analysis. *Water Resources Management* **24** (10), 2365–2380. doi:10.1007/s11269-009-9556-5.

MoFA 2011 *Facts and Figures (2010)*. Ministry of Food and Agriculture (MoFA), Statistics, Research and Information Directorate (SRID), Accra.

Mora, C. F. A. G., Longman, R. J., Dacks, R. S., Walton, M. M., Tong, E. J., Sanchez, J. J., Kaiser, L. R., Stender, Y. O., Anderson, J. M., Ambrosino, C. M., Fernandez-Silva, I., Giuseffi, L. M. & Giambelluca, T. W. 2013 The projected timing of climate departure from recent variability. *Nature* **502**, 183–187.

Moriasi, D. N., Arnold, J. G., Van Liew, M. W., Bingner, R. L., Harmel, R. D. & Veith, T. L. 2007 Model evaluation guidelines for systematic quantification of accuracy in watershed simulations. *American Society of Agricultural and Biological Engineers* **50** (3), 885–900.

Muthee, K. W., Mbow, C., Macharia, G. M. & Leal-Filho, W. 2018 Ecosystem services in adaptation projects in West Africa. *International Journal of Climate Change Strategies and Management* **10** (4), 533–550.

Niang, I., Ruppel, O. C., Abdrabo, M. A., Essel, A., Lennard, C., Padgham, J. & Urquhart, P. 2014 Africa. In: *Climate Change 2014: Impacts, Adaptation, and Vulnerability. Part B: Regional Aspects. Contribution of Working Group II to the Fifth Assessment Report of the Intergovernmental Panel on Climate Change* (V. R. Barros, C. B. Field, D. J. Dokken, M. D. Mastrandrea, K. J. Mach, T. E. Bilir, M. Chatterjee, K. L. Ebi, Y. O. Estrada, R. C. Genova, B. Girma, E. S. Kissel, A. N. Levy, S. MacCracken, P. R. Mastrandrea & L. L. White, eds). Cambridge University Press, Cambridge, pp. 1199–1265.

Nicholson, S. E. & Webster, P. J. 2007 A physical basis for the inter annual variability of rainfall in the Sahel. *Quarterly Journal of the Royal Meteorological Society* **133**, 2065–2084.

Nikiema, P. M., Sylla, M. B., Ogunjobi, K., Kebe, I., Gibbaa, P. & Giorgid, F. 2016 Multi-model CMIP5 and CORDEX simulations of historical summer temperature and precipitation variabilities over West Africa. *International Journal of Climatology*. doi:10.1002/joc.4856.

Nutsukpo, D. K., Jalloh, A., Zougmoré, R., Nelson, G. C. & Thomas, T. S. 2013 Ghana. In: *West African Agriculture and Climate Change: A Comprehensive Analysis*. Chapter 6. International Food Policy Research Institute, Washington, D.C., pp. 141–172. Available from: http://ebrary.ifpri.org/cdm/ref/collection/p15738coll2/id/127450 (accessed 3 January 2018).

Obuobie, E., Kankam-Yeboah, K., Amisigo, B., Opoku-Ankomah, Y. & Ofori, D. 2012 Assessment of water stress in river basins in Ghana. *Journal of Water and Climate Change* **03** (4), 276–286. doi:10.2166/wcc.2012.030.

Oliver, M. A. & Webster, R. 1990 Kriging: a method of interpolation for geographical information systems. *International Journal of Geographical Information Systems* **4** (3), 313–332.

Paeth, H., Hall, N. M. J., Gaertner, M. A., Alonso, M. D., Moumouni, S., Polcher, J., Ruti, P. M., Fink, A. H., Gosset, M., Lebel, T., Gaye, A. T., Rowell, D. P., Moufouma-Okia, W., Jacob, D., Rockel, B., Giorgi, F. & Rummukainen, M. 2011 Progress in regional downscaling of West African precipitation. *Atmospheric Science Letters* **12** (1), 75–82. doi:10.1002/asl.306.

Preethi, B. & Revadekar, J. V. 2013 Kharif foodgrain yield and daily summer monsoon precipitation over India. *International Journal of Climatology* **33**, 1978–1986. doi:10.1002/joc.3565.

Rasul, G., Chaudhry, Q. Z., Mahmood, A. & Hyder, K. W. 2011 Effect of temperature rise on crop growth and productivity. *Pakistan Journal of Meteorology* **8** (15), 53–62.

Samuelsson, P., Jones, C. G., Willén, U., Ullerstig, A., Gollvik, S., Hansson, U., Jansson, C., Kjellström, E., Nikulin, G. & Wyser, K. 2011 The Rossby Centre Regional Climate model RCA3: model description and performance. *Tellus A: Dynamic Meteorology and Oceanography* **63** (1), 4–23. doi:10.1111/j.1600-0870.2010.00478.x.

Semenov, M. A. & Stratonovitch, P. 2010 Use of multi-model ensembles from global climate models for assessment of climate change impacts. *Journal of Climate Research* **41** (1), 1–14. doi:10.3354/cr00836.

Serdeczny, O., Adams, S., Baarsch, F., Coumou, D., Robinson, A., Hare, W., Schaeffer, M., Perrette, M. & Reinhardt, J. 2016 Climate change impacts in Sub-Saharan Africa: from physical changes to their social repercussions. *Regional Environmental Change*. doi:10.1007/s10113-015-0910-2.

Souvignet, M., Gaese, H., Ribbe, L., Kretschmer, N. & Oyarzún, R. 2010 Statistical downscaling of precipitation and temperature in north-central Chile: an assessment of possible climate change impacts in an arid Andean watershed. *Hydrological Sciences Journal* **55** (1), 41–57. doi:10.1080/02626660903526045.

Teutschbein, C. & Seibert, J. 2012 Bias correction of regional climate model simulations for hydrological climate-change impact studies: review and evaluation of different methods. *Journal of Hydrology* **456–457**, 12–29.

Thomson, M. C., Muñoz, A. G., Cousin, R. & Shumake-Guillemot, J. 2018 Climate drivers of vector-borne diseases in Africa and their relevance to control programmes. *Infectious Diseases of Poverty* **7**, 81. doi:10.1186/s40249-018-0460-1.

UNEP 2002 *Africa Environment Outlook: Past, Present and Future Perspectives*. United Nations Environment Programme (UNEP), Nairobi, Kenya.

UNEP 2017 *Country Level Impacts of Climate Change (CLICC) Pilot Project – Ghana*. United Nations Environment Programme (UNEP). Available from: https://uneplive.unep.org/media/docs/theme/13/clicc_pilot_ghana.pdf (accessed 15 March 2019).

UPEI 2017 Island Database. Climate Records for the Day, and Other Database Information. Available from: https://climate.upei.ca (accessed 15 February 2017).

Vischel, T. & Lebel, T. 2007 Assessing the water balance in the Sahel: impact of small scale rainfall variability on runoff. Part 2: idealized modeling of runoff sensitivity. *Journal of Hydrology* **333** (2–4), 340–355. doi:10.1016/j.jhydrol.2006.09.007.

Welborn, L. 2018 *Climate Change and Poverty in Africa*. Institute for security studies (ISS). Available from: https://issafrica.org/iss-today/climate-change-and-poverty-in-africa (accessed 12 May 2019).

Wilby, R. L. & Dawson, C. W. 2004 *Using SDSM Version 3.1 d a Decision Support Tool for the Assessment of Regional Climate Change Impacts. User Manual*.

Wilby, R. L. & Dawson, C. W. 2013 The Statistical DownScaling Model (SDSM): insight from one decade of application. *International Journal of Climatology* 33 (7), 1707–1719. doi:10.1002/joc.3544.

Wilby, R. L., Dawson, C. W. & Barrow, E. M. 2002 SDSM decision support tool for the assessment of regional climate change impacts. *Environmental Modeling & Software* **17** (2), 147–159.

Wilby, R. L., Dawson, C. W., Murphy, C., O'Conner, P. & Hawkins, E. 2014 The Statistical DownScaling model – Decision Centric (SDSM-DC): conceptual basis and applications. *Climate Research* **61**, 251–268.

WRC 2012 *Pra River Basin – Integrated Water Resources Management Plan*. Water Resources Commission (WRC), Accra, p. 53.

Xystrakis, F., Kallimanis, A. S., Dimopoulos, P., Halley, J. M. & Koutsias, N. 2014 Precipitation dominates fire occurrence in Greece (1900–2010): its dual role in fuel build-up and dryness. *Natural Hazards and Earth System Science* **14**, 21–32. doi:10.5194/nhess-14-21-2014.

First received 17 October 2018; accepted in revised form 4 July 2019. Available online 29 July 2019